ACOUSTICAL LETTER

A method for structural intensity measurement on a plate by using the spectral element method

Tetsuo Oya[1,*], Yôiti Suzuki[1,†] and Koichi Ito[2,‡]

[1]*Research Institute of Electrical Communication and Graduate School of Information Sciences, Tohoku University, 2–1–1 Katahira, Aoba-ku, Sendai, 980–8577 Japan*
[2]*M&M Research, 4–15–3 Jingumae, Shibuya-ku, Tokyo, 150–0001 Japan*

(*Received 10 November 2004, Accepted for publication 1 December 2004*)

Keywords: Structural intensity, Measurement, Spectral element method
PACS number: 43.40.Yq [DOI: 10.1250/ast.26.301]

1. Introduction

Structural intensity is defined as a vectorial quantity which represents the mechanical power flow of vibrating elastic structures. Distribution of structural intensity exhibits propagation paths of vibration power, and thus it can be an effective tool for vibration and noise reduction. Many studies on structural intensity concerning measurement [1,2] and its characteristics and precision [3–5] have been conducted. Some problems, however, have prevented the measurement of structural intensity from being practically applied. The majority of research to date on the measurement of structural intensity has been conducted using the finite difference method. The formula of structural intensity consists of higher order derivatives of space, and thus, error inevitably arises from the finite difference method. Moreover, a huge number of measurement points should be reduced for practical use. Although other methods [6–8] have been presented, there are still problems with regard to their accuracy or the number of measurement points.

In this paper, SEM (Spectral Element Method) [9] is applied to develop a new method for structural intensity measurement. In SEM, shape function is made by exact solution and therefore has an advantage in the interpolation of a harmonically vibrating field. By combining SEM and actual measurement, structural intensity distribution can be more accurately obtained with a relatively small number of measurement points. The validity of the proposed method is examined by numerical simulations performed on a plate structure under the assumption of far field.

2. Structural intensity

Structural intensity is defined as the vibrational power per unit width of the central surface of a structure. For flat structures such as a straight beam or plate, only flexural motion is used to calculate structural intensity because this motion surpasses other modes of deformation. In this paper, our interest is focused on a uniform flat plate. First, density of structural intensity $\boldsymbol{i}$ is defined at every point of the volume as a three-dimensional vector:

$$\boldsymbol{i} = -\boldsymbol{\sigma} \cdot \boldsymbol{v}, \tag{1}$$

where $\boldsymbol{\sigma}$ is a stress tensor and $\boldsymbol{v}$ is a velocity vector. This is a Poynting vector in a linear elastic body [10]. Structural intensity is a resultant of this vector over the cross section of the structure. Therefore, structural intensity $\boldsymbol{I}$ is a two-dimensional vector expressing a vibrational power at the central surface:

$$\boldsymbol{I} = -\int_{-\frac{h}{2}}^{\frac{h}{2}} \boldsymbol{\sigma} \cdot \boldsymbol{v} dz. \tag{2}$$

This expression is denoted in tensor form and its physical component for a system with arbitrary coordinates is necessary for practical use. Converted to the Cartesian coordinate system, this is identical to Romano's expression [11]. In this paper, the expression of structural intensity in the flexural mode for a plate [2] is employed. Practically, active structural intensity is used to evaluate actual power flow.

3. Methodology

3.1. Spectral element for a plate

In our approach to obtain structural intensity vectors by measurement, the SEM was applied to a plate structure. This method was presented by Doyle [9] to compute the behavior of beams and a plate by developing a spectrally formulated finite element termed the spectral element. One of the advantages of this method is that a vibrational field is easily interpolated by the spectral element because its shape function is derived using a wave solution. Therefore, wave propagation between discontinuities can be predicted precisely. However, for the sake of measurement, this advantage will be reduced slightly, since, in our procedure, nodal variables of the spectral element are obtained by measuring them and there could be some frequency dependent limitation of element size. Nevertheless, this approach is still useful since its shape function can be directly derived from the wave solution with a relatively smaller number of degrees of freedom in a system equation.

The method begins with the equation of motion of a thin plate for displacement $\bar{w}$,

$$D\nabla^4 \bar{w} + \rho h \ddot{\bar{w}} = 0, \tag{3}$$

*e-mail: oya@ais.riec.tohoku.ac.jp
†e-mail: yoh@ais.riec.tohoku.ac.jp
‡e-mail: ito@m-reserch.co.jp

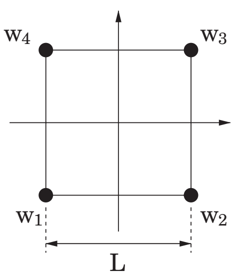

Fig. 1 Plate element for measurement with size L.

where D is the plate-bending stiffness, ρ is the density and h is the thickness. With the general solution $\bar{w}(x,y,t) = we^{ik_x x}e^{ik_y y}e^{i\omega t}$, the following characteristic relation is obtained:

$$D(k_x^2 + k_y^2)^2 - \rho h\omega^2 = 0, \tag{4}$$

where k_x and k_y are wavenumbers in directions x and y, respectively, and ω is the angular frequency. Transforming the wavenumbers into polar coordinates,

$$\kappa^2 = k_x^2 + k_y^2, \quad k_x = \pm\kappa\cos\theta \quad \text{and} \quad k_x = \pm\kappa\sin\theta, \tag{5}$$

where κ denotes the absolute value of the wavenumber in polar coordinate and θ means the azimuth angle of the direction of the wave propagation in κ-space. Although Eq. (5) has four roots, two real roots are employed because of the assumption of far field. One can obtain the far field solution of the plate by combining each term with arbitrary constants. Setting a square region of size L on a plate (Fig. 1), the displacement of the plate is expressed as

$$\begin{aligned} w(x,y) &= Ae^{-i\left(\kappa\cos\theta\left(\frac{L}{2}+x\right)+\kappa\sin\theta\left(\frac{L}{2}+y\right)\right)} \\ &\quad + Be^{-i\left(\kappa\cos\theta\left(\frac{L}{2}+x\right)+\kappa\sin\theta\left(\frac{L}{2}-y\right)\right)} \\ &\quad + Ce^{-i\left(\kappa\cos\theta\left(\frac{L}{2}-x\right)+\kappa\sin\theta\left(\frac{L}{2}+y\right)\right)} \\ &\quad + De^{-i\left(\kappa\cos\theta\left(\frac{L}{2}-x\right)+\kappa\sin\theta\left(\frac{L}{2}-y\right)\right)} \\ &= \boldsymbol{NC}, \end{aligned} \tag{6}$$

where $\boldsymbol{N}$ is the interpolation function of the plate and $\boldsymbol{C}$ is the matrix of the constants. The SEM procedure is applied to relate the coefficients of Eq. (6) to the displacements of the region. In a measurement, these displacements of each grid point are interpreted as nodal displacement of the element. Let the displacement vector obtained by a measurement be $\boldsymbol{q}$, which can be expressed with $\boldsymbol{C}$:

$$\boldsymbol{q} = \boldsymbol{N}_L\boldsymbol{C} \Rightarrow \boldsymbol{C} = \boldsymbol{N}_L^{-1}\boldsymbol{q}, \tag{7}$$

where $\boldsymbol{N}_L$ is the matrix constructed by substituting nodal coordinates into $\boldsymbol{N}$. Consequently, displacement of the plate is expressed as

$$\begin{aligned} w(x,y) &= \boldsymbol{NC} = \boldsymbol{N}(x,y,\theta)\boldsymbol{N}_L^{-1}(\theta)\boldsymbol{q} \\ &= \boldsymbol{N}_K\boldsymbol{q}, \end{aligned} \tag{8}$$

where $\boldsymbol{N}_K$ is the interpolation function of the plate element under the assumption of far field.

3.2. Determination of argument θ

In the displacement function Eq. (8), angle θ is a variable which is still unknown. To determine it, the energy conservation is employed. If there is no dissipation or external force, in a harmonic vibration, time-averaged strain energy and kinetic energy should be identical even in the plate element. The element's strain energy $\boldsymbol{U}_T$ and kinetic energy $\boldsymbol{T}_T$ are

$$\boldsymbol{U}_T = \frac{1}{2}\tilde{\boldsymbol{q}}\boldsymbol{K}(\theta)\boldsymbol{q}, \tag{9}$$

$$\boldsymbol{T}_T = \frac{1}{2}\tilde{\dot{\boldsymbol{q}}}\boldsymbol{M}(\theta)\dot{\boldsymbol{q}}, \tag{10}$$

where $\tilde{}$ denotes the conjugate transposed matrix, $\boldsymbol{K}$ is the stiffness matrix and $\boldsymbol{M}$ is the mass matrix of the element. $\boldsymbol{U}_T$ and $\boldsymbol{T}_T$ are used to determine angle θ because these are functions of θ and are identical to each other at the true θ.

4. Numerical analysis as a test case

With using a complete solution of plate including near field, the proposed method is carried out to confirm the validity of the procedure. This field is assumed to be a steel plate with the following physical constants: Young's modulus $= 2.1 \times 10^{11}$ [Pa], density $= 7{,}860\,\text{kg/m}^3$, Poisson's ratio 0.3 and thickness 0.001 [m].

As an example case, the true value of θ is set at $\frac{\pi}{3}$ and this value is calculated from four nodal displacements by the proposed method. The error between true value and computed one is then considered with respect to both angle θ and structural intensity. Structural intensity is converted to the absolute value of the vector and averaged at four points:

$$\left(-\frac{L}{4}, -\frac{L}{4}\right), \quad \left(\frac{L}{4}, -\frac{L}{4}\right), \quad \left(\frac{L}{4}, \frac{L}{4}\right), \quad \left(-\frac{L}{4}, \frac{L}{4}\right).$$

Figure 2 is the strain energy and the kinetic energy as a function of θ in the case that frequency is 100 Hz. This figure depicts that strain energy crosses kinetic energy at the point very close to the true $\theta = 1.0472$.

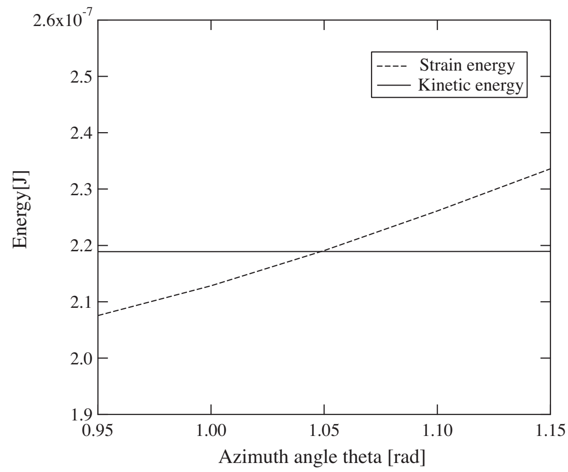

Fig. 2 Strain energy and kinetic energy as a function of argument θ for the case that frequency is 100 Hz and element size is 0.03 [m].

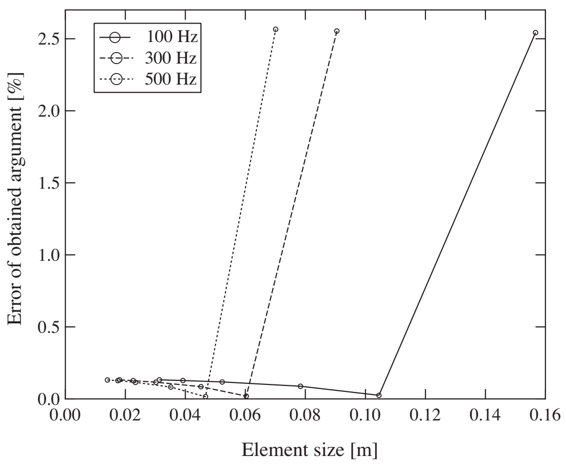

Fig. 3 Error between the true θ and the computed one. Circles on the lines denote one-tenth, one-eighth, one-sixth, one-fourth, one-third and one-half of the wavelength.

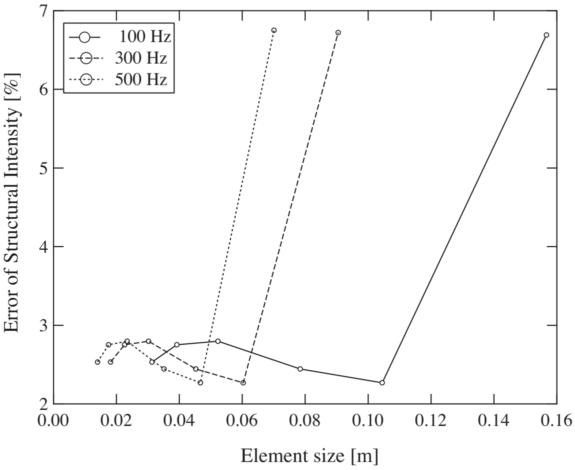

Fig. 4 Error between the true structural intenisty and the computed one. Circles on the lines denote one-tenth, one-eighth, one-sixth, one-fourth, one-third and one-half of the wavelength.

Figure 3 shows that the errors between the true θ and the computed one are very small when the element size is smaller than one third of the wavelength for each frequency. However, error becomes large when the size is close to half of wavelength.

Figure 4 describes that the errors of computed structural intensity are within 2 or 3% and as the element size approaches to a half of wavelength the error becomes large. This result is resonable because of the influence of the error of computed θ. These results show that the method provides accurate measurement results so long as the element size is shorter than one third of wavelength.

5. Simulation using the Finite Element Method

MSC.MARC is employed to model the cantilever steel plate (2 [m] $\times$ 0.1 [m]) shown in Fig. 5. The number of elements used is 1280 and the bilinear thin-shell element

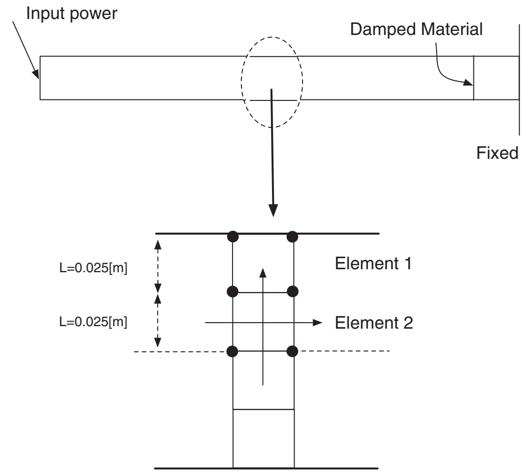

Fig. 5 Cantilever plate with a load and fixed displacement.

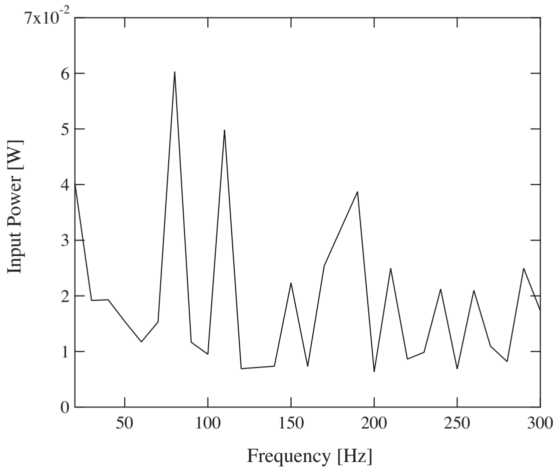

Fig. 6 Input power of the model structure.

(No. 139) is employed. An external load is applied in the thickness direction with 1 [N] and the other side is fixed. A numerical damping factor is given in 64 elements near the fixed edge to generate power flow. Physical constants are same as in the previous section. To consider far field, central elements are used for evaluation. The size of the element for measurement is 0.025 [m].

In this simulation, the exact values of θ are not clear. Thus, power evaluation is performed by comparing the input power by the external load and the total power flow crossing the center line of this model. Four elements are used in the width direction and half of them are used for evaluation because of symmetry at lower frequencies.

Figures 6 and 7 show the input power and the total power of the model, respectively. Figure 8 depicts that the error between the input power and the total power is very small. Thus, computed θ must be close to its exact value.

6. Conclusion

The new method for structural intensity measurement was studied. The formulation was done by using the concept of SEM. To determine the unknown variable, the energy

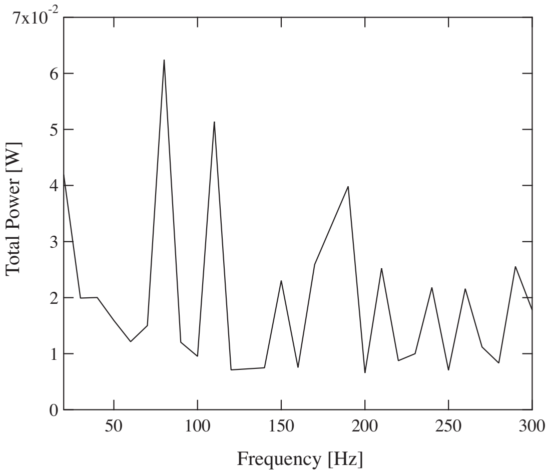

Fig. 7 Total power through the center line of the model structure.

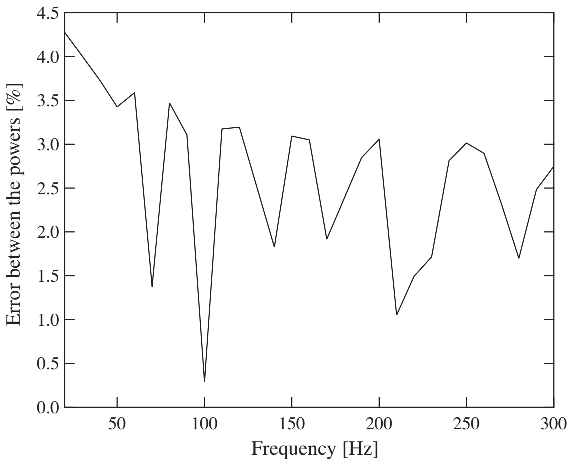

Fig. 8 Errors between the input power and the total power.

conservation relation of the element was employed. In the analysis using the complete solution of a plate, the unknown value was successfully obtained. In the simulation using FEM, a finite element model was used as a reference structure and the proposed method worked well to compute the structural intensity within a small error.

References

[1] D. U. Noiseux, "Measurement of power flow in uniform beams and plates," *J. Acoust. Soc. Am.*, **47**, 238–247 (1970).

[2] G. Pavić, "Measurement of structure borne wave intensity. Part I. Formulation of the methods," *J. Sound Vib.*, **49**, 221–230 (1976).

[3] R. Nishimura, Y. Iwaya, Y. Suzuki and T. Sone, "Decaying wave component of one-dimensional vibration intensity," *J. Acoust. Soc. Jpn.* (*J*), **51**, 763–768 (1995).

[4] Y. Iwaya, Y. Suzuki, M. Sakata and T. Sone, "Influence of the terminating impedance of a semi-infinite beam on the reflection of bending wave and vibration intensity," *J. Acoust. Soc. Jpn.* (*J*), **56**, 243–248 (2000).

[5] K. Shibata, M. Kato, N. Takatsu, O. Wakatsuki and K. Kobayashi, "Measuring condition and precision of structural intensity measurement," *Proc. Inter-Noise 94*, Yokohama, Japan, pp. 1697–1700 (1994).

[6] R. Morikawa, S. Ueha and K. Nakamura, "Error evaluation of the structural intensity measured with a scanning laser Doppler vibrometer and a *k*-space signal processing," *J. Acoust. Soc. Am.*, **99**, 2913–2921 (1996).

[7] C. R. Halkyard and B. R. Mace, "A Fourier series approach to the measurement of flexural wave intensity in plates," *J. Sound Vib.*, **203**, 101–126 (1997).

[8] K. Saijou and S. Yoshikawa, "Structural intensity measurement of cylindrical shell based on NAH technique and influences of a rib on the acoustic energy flow," *J. Acoust. Soc. Jpn.* (*E*), **20**, 125–136 (1999).

[9] J. F. Doyle, *Wave Propagation in Structures* (Springer-Verlag, New York, 1997).

[10] B. A. Auld, *Acoustic Fields and Waves in Solids*, 2nd ed. (Robert E. Krieger Publishing Company Inc., Melbourne, Fla., 1990), Chap. 5.

[11] A. J. Romano, P. B. Abraham and E. G. Williams, "A Poynting vector formulation for thin shells and plates, and its application to structural intensity analysis and source localization. Part I: Theory," *J. Acoust. Soc. Am.*, **87**, 1166–1175 (1990).